A Convergent Approach to Protein Design. Metal Ion-Assisted Spontaneous Self-Assembly of a Polypeptide into a Triple-Helix Bundle Protein†

M. Reza Ghadiri,*,‡ Christopher Soares, and Chong Choi

Contribution from the Departments of Chemistry and Molecular Biology, The Scripps Research Institute, La Jolla, California 92037. *Received February 8, 1991*

Abstract: A novel metal ion-assisted self-organizing molecular process is described by which a small peptide has been assembled into a large and topologically predetermined protein tertiary structure. The intrinsic binding energy of a metal ion coordination complex as well as the stringent geometrical requirements present for a strong metal ion–ligand interaction has been exploited to control the oligomeric state as well as the relative orientation of peptide subunits participating in an intermolecular assembly process. A 15-residue amphiphilic peptide with a 2,2′-bipyridine functionality at the N-terminus was designed and shown to undergo spontaneous self-assembly, in the presence of transition metal ions, to form a 45-residue triple-helical coiled-coil metalloprotein.

Despite the accumulation of a large body of information about protein structures,[1] de novo design of artificial proteins remains an elusive task.[2] The major obstacle in the design of proteins from linear polypeptide sequences is the lack of comprehensive understanding of how the one-dimensional sequence information directs the formation of a discrete three-dimensional state of a protein. An alternative approach for the construction of artificial proteins might be to develop *self-organizing molecular processes* by which small peptides can be assembled into large and topologically predetermined protein tertiary structures. Here we report for the first time a metal ion-assisted self-assembly process for the construction of an artificial protein.[3] A 15-residue amphiphilic peptide with a 2,2′-bipyridine functionality at the N-terminus was designed and shown to undergo spontaneous self-assembly, in the presence of transition metal ions, to form a 45-residue triple-helical coiled-coil metalloprotein.

Short peptides capable of forming amphiphilic secondary structures possess solution properties which are particularly well-suited for use in protein design.[4] Typically, when an amphiphilic peptide is dissolved in an aqueous solution, an equilibrium between peptide monomer and various intermolecular aggregates is established. However, designing an amphiphilic peptide which can self-assemble into a specific and topologically predetermined ensemble is extremely difficult and requires accurate assessment of the relative binding energy of the large number of possible intermolecular associations.[2c] Therefore, the utility of amphiphilic secondary structure building blocks in the construction of artificial proteins depends ultimately on controlling the number, as well as the relative spatial orientation, of the subunits participating in the assembly process. Here we present a novel approach in which the oligomeric state of the polypeptide and the overall topology of the protein are manipulated by exploiting the interaction of a metal ion with an appropriately designed metal ion binding site.

Design Principles. In a fashion similar to our recent studies in the design of metal ion stabilized α-helical peptides,[5] we envisioned that the intrinsic binding energy of a metal ion coordination complex might be effective in the design and construction of artificial proteins. It was further postulated that the stringent geometrical requirements present for a strong metal ion–ligand interaction would be highly effective in controlling the oligomeric state as well as the relative orientation of peptide subunits participating in the intermolecular assembly process. According to our hypothesis, a metal ion-assisted self-assembly process must in general comply with the following design principles. (a) The peptide subunits participating in the self-assembly process must each donate at least one ligand to the putative metal ion binding site. (b) Amphiphilic peptides must be designed in a way that only when the subunits assume the desired relative orientation would the ligands be close enough in space to interact cooperatively with a metal ion. In other words, the metal ion binding site must exclude or disfavor other tertiary structure arrangements. (c) The metal complex should have a high formation constant to be able to significantly contribute to the overall thermodynamic stability of the desired ensemble. In addition, in order to simplify the isolation, purification, and physicochemical characterization of the resulting protein ensemble, it is preferred that the metalloprotein also exhibit high kinetic stability. Therefore, whenever possible, the use of exchange-inert metal complexes[6] must be emphasized.

Design of an Artificial Triple-Helix Metalloprotein. In order to evaluate the utility of metal ions in self-assembly processes, we chose to design a parallel triple-helix bundle protein. Only a few examples of triple-stranded α-helical coiled-coil motifs have been observed and are generally made up of homo- or heterotrimers of 52 to 160 amino acid long helical segments.[7] Although generalizations regarding sequence requirements have not yet been established, helical trimers have been found to contain several somewhat imperfect heptad repeats. Several factors were considered in order to allow an unbiased assessment of our design

† This paper is dedicated to Professor Barry M. Trost on the occasion of his 50th birthday.

‡ Searle Scholar, 1991–1994; Beckman Young Investigator, 1991–1993.

(1) (a) Richardson, J. S. *Adv. Protein Chem.* **1981**, *34*, 167. (b) *Prediction of Protein Structure and the Principles of Protein Conformation*; Fasman, G. D., Ed.; Plenum Press: New York, 1989.

(2) (a) Richardson, J. S.; Richardson, D. C. *Trends Biochem. Sci.* **1989**, *14*, 304. (b) Mutter, M.; Vuilleumier, S. *Angew. Chem., Int. Ed. Engl.* **1989**, *5*, 535. (c) Hill, C. P.; Anderson, D. H.; Wesson, L.; DeGrado, W. F.; Eisenberg, D. *Science* **1990**, *249*, 543. (d) Ho, S. P.; DeGrado, W. F. *J. Am. Chem. Soc.* **1987**, *109*, 6751. (e) Hecht, M. H.; Richardson, J. S.; Richardson, D. C.; Ogden, R. C. *Science* **1990**, *249*, 884. (f) Regan, L.; DeGrado, W. F. *Science* **1988**, *241*, 976. (g) Hahn, K. W.; Wieslaw, A. K.; Stewart, J. M. *Science* **1990**, *248*, 1544. (h) Kaumaya, P. T. P.; Berndt, K. D.; Heidorn, D. B.; Trewhella, J.; Kedzdy, F. J.; Goldberg, E. *Biochemistry* **1990**, *29*, 13. (i) Handel, T.; DeGrado, W. F. *J. Am. Chem. Soc.* **1990**, *112*, 6710.

(3) For the use of metal ion complexation in self-assembly processes see: (a) Koert, V.; Harding, M. M.; Lehn, J. M. *Nature* **1990**, *346*, 339. (b) Constable, E. C.; Elder, S. M.; Healy, J.; Ward, M. D.; Tocher, D. A. *J. Am. Chem. Soc.* **1990**, *112*, 4590.

(4) (a) Kaiser, E. T.; Kezdy, F. J. *Science* **1984**, *223*, 249. (b) Taylor, J. W.; Kaiser, E. T. *Pharmacol. Rev.* **1986**, *38*, 291. (c) DeGrado, W. F.; Lear, J. D. *J. Am. Chem. Soc.* **1985**, *107*, 7684.

(5) (a) Ghadiri, M. R.; Choi, C. *J. Am. Chem. Soc.* **1990**, *112*, 1630. (b) Ghadiri, M. R.; Fernholz, K. A. *J. Am. Chem. Soc.* **1990**, *112*, 9633. Also see: Ruan, F.; Chen, Y.; Hopkins, P. B. *J. Am. Chem. Soc.* **1990**, *112*, 9403.

(6) For the earliest definition see: Taube, H. *Chem. Rev.* **1952**, *50*, 69. Also see: Van Wart, H. E. *Methods Enzymol.* **1988**, *158*, 95.

(7) (a) Wilson, I. A.; Skebel, J. J.; Wiley, D. C. *Nature* **1981**, *289*, 366. (b) Doolittle, R. F.; Goldbaum, D. M.; Dolittle, L. R. *J. Mol. Biol.* **1978**, *120*, 311. (c) Kodama, T.; Freeman, M.; Rohrer, L.; Zabrecky, J.; Matsudaira, P.; Krieger, M. *Nature* **1990**, *343*, 531. (d) Cohen, C.; Parry, D. A. D. *Proteins* **1990**, *7*, 1.

0002-7863/92/1514-825$03.00/0 © 1992 American Chemical Society

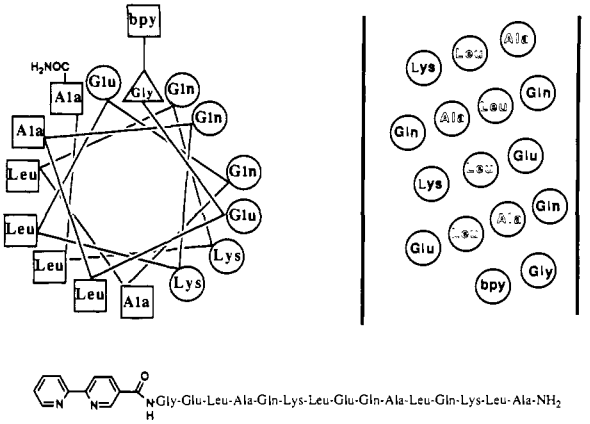

Figure 1. Helical wheel and net diagrams of the bpy-peptide subunit (top) illustrating the segregation of hydrophobic and hydrophilic residues. Peptide sequence is shown at the bottom.

principles. To avoid predisposition toward triple-helix formation, the putative α-helical segment was limited to four helical turns. While such a short amphiphilic helix can, in principle, participate in various multimeric aggregates, it is not long enough to form stable three-stranded α-helical coiled-coil topology in the absence of other stabilizing interactions. Furthermore, while the peptide sequence was designed to be compatible with parallel triple-helical structure (vide infra), it does not conform to the heptad repeats implicated in α-helical coiled-coil structures.

The 15-residue polypeptide depicted in Figure 1 was designed to serve as the putative amphiphilic α-helical building block. The peptide is composed primarily of five amino acid residues which strongly favor helix formation.[8] Polar and nonpolar residues are segregated and each occupy half of the helix surface. Leucine and alanine residues constitute the hydrophobic face while glutamic acid, lysine, and glutamine side chain functionalities comprise the remaining hydrophilic surface. In order to maximize favorable charge–helix dipole interactions and enhance helix stability, the peptide was blocked at the chain ends and lysine and glutamic acid residues were placed near the C- and N-termini, respectively.[9] The design of the peptide sequence was aided by examining a CPK model of a triple-helical coiled-coil structure. Interhelical packing of nonpolar side chains which form the hydrophobic core of the structure was evaluated and the amino acid sequence was designed accordingly to afford a sterically favored packing arrangement. Although optimal hydrophobic packing is believed to be essential for the stability of a globular structure, we avoided overdesign on the basis of the static model at hand. In addition, the solvent exposed hydrophilic surface was designed to encourage several possible intrahelical as well as interhelical electrostatic interactions. Glycine was used as a conformationally flexible spacer connecting the metal binding site to the putative helical domain. We believe that such a convergent approach to protein design is particularly well-suited for rapid structural evaluation and optimization.

In order to preserve the overall C_3 symmetry of the triple-stranded topology, each α-helical subunit was designed to donate a bidentate ligand to the putative octahedral metal ion coordination site. Among various bidentate ligands, the 2,2′-bipyridyl moiety seemed to offer the most desirable physicochemical properties for the triple-stranded topology. 2,2′-Bipyridyl ligands readily react with a variety of transition metal ions to form well-characterized tris-chelated complexes. Most importantly, tris-bipyridyl complexes possess high thermodynamic and kinetic stabilities required for the formation and isolation of the desired intermolecular ensemble.[10] Furthermore, the bipyridyl chromophore also serves as a useful spectroscopic probe for gaining further insight into the efficacy of the design (vide infra). In addition, the photochemical and electron transfer properties of bipyridine–metal complexes can set the stage for the future design of catalytically active proteins. In order to simplify both design and synthesis, the metal binding site was placed at the N-termini of the triple-helical structure. Analysis of the X-ray structures of tris-bipyridine–metal complexes[11] and the CPK model of the putative triple-helical protein indicated that attaching the bipyridyl ligand through its C-5 position to the helical segment minimizes steric congestion and ligand–ligand repulsions during the assembly process.

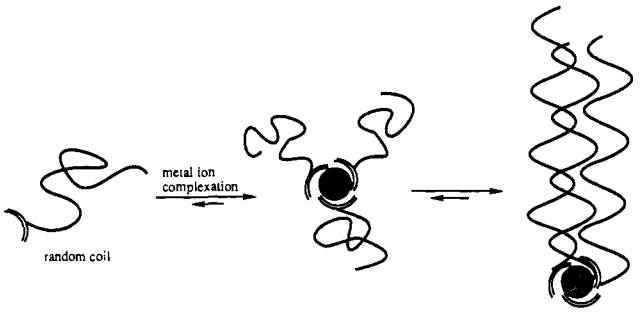

Figure 2. Hypothetical folding pathway illustrated for the metal ion-assisted self-assembly of a triple-helix bundle metalloprotein. Double circular arcs represent the bipyridyl–metal binding sites.

The 15-residue polypeptide (Figure 1) ending with the penultimate glycine residue was chemically synthesized on a benzhydrylamine resin by standard Merrifield solid-phase methodology.[22] The terminal amino functionality of the peptide was deprotected and then coupled with 5-carboxy-2,2′-bipyridine, prepared according to eq 1, using the standard DCC-Hobt method. Treatment with anhydrous HF afforded a crude peptide which was purified by RP HPLC and characterized by amino acid analysis and mass spectroscopy.

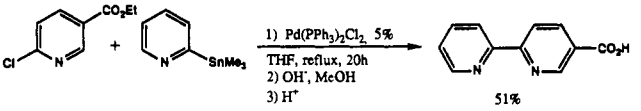

(1)

The decisive role which the metal ion complexation plays in controlling the number of subunits participating in the assembly process as well as the overall topology of the resulting ensemble can be illustrated by analyzing the hypothetical two-step folding mechanism shown in Figure 2 for the self-assembly of the triple-helix bundle metalloprotein. According to the scheme, metal ion complexation initially sequesters three peptide chains to form the putative intermediate shown thereby biasing the system toward the trimeric ensemble. The binding energy of the metal ion complexation not only drives the formation of the intermediate but also compensates for the loss of entropy associated with the spatial organization of the peptide subunits. As compared to the free amphiphilic peptide, the intermediate specie possesses higher coil density as well as dramatically greater effective concentration of hydrophobic residues. The short-range interactions induced by the metal ion complexation should then strongly favor intramolecular rather than intermolecular hydrophobic interactions. Consequently, the intermediate specie undergoes a hydrophobic collapse to yield the desired triple-helical bundle topology.

(8) Chou, P. Y.; Fasman, G. D. *Annu. Rev. Biochem.* **1978**, *47*, 251.
(9) (a) Blagdon, D. E.; Goodman, M. *Biopolymers* **1975**, *14*, 241. (b) Richardson, J. S.; Richardson, D. C. *Science* **1988**, *240*, 1648. (c) Presta, L. G.; Rose, G. D. *Science* **1988**, *240*, 1632. (d) Shoemaker, K. R.; Kim, P. S.; Brems, D. N.; Marqusee, S.; York, E. J.; Chaiken, I. M.; Stewart, J. M.; Baldwin, R. L. *Proc. Natl. Acad. Sci. U.S.A.* **1985**, *82*, 2349.
(10) (a) *Guide to Stability Design Criteria for Metal Structures*; Galambos, T. V., Ed.; Wiley: New York, 1988. (b) *Stability Constants of Metal-Ion Complexes IUPAC*; Permagon Press: New York, 1979–1982.
(11) (a) Constable, E. C.; Raithby, P. R.; Smit, D. N. *Polyhedron* **1989**, *8*, 367. (b) Hauser, A.; Mader, M.; Robinson, W. T.; Murugesan, R.; Ferguson, J. *Inorg. Chem.* **1987**, *26*, 1331.
(12) Mason, S. F. *Inorg. Chem. Acta* **1968**, 89.
(13) Katta, V.; Chowdhury, S. K.; Chait, B. T. *J. Am. Chem. Soc.* **1990**, *112*, 5348.

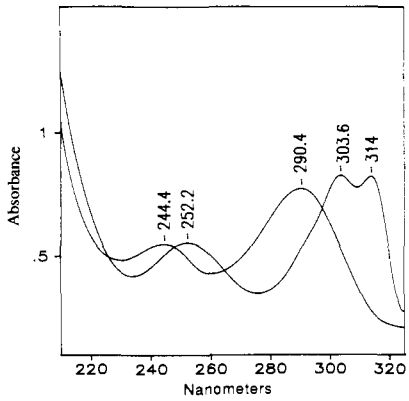

Figure 3. Plot of absorbance vs wavelength for the peptide (21.2×10^{-6} M in 5 mM sodium borate, pH 6.4 at 20.8 °C) in the absence and presence of 31×10^{-6} M $NiCl_2$.

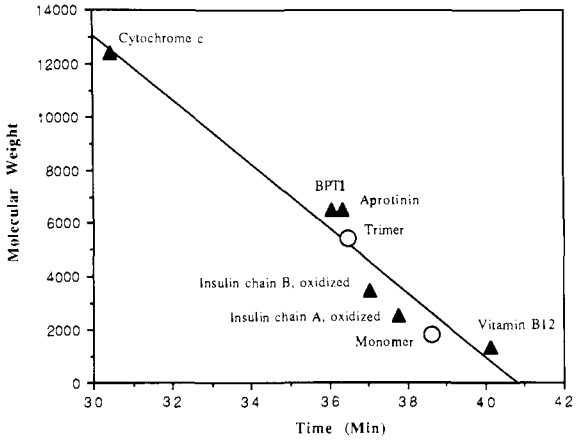

Figure 4. Calibration curve for a Superose 12 HR 10/30 column (Pharmacia). All samples were run in 6 M guanidine–HCl, 50 mM sodium borate pH 7.1, with a flow rate of 0.4 mL/min, and detected at 280 nm. Triple helix in the presence of Ni^{2+} or Co^{2+}, estimated MW = 5260 and calculated MW = 5522.

Results and Discussion

Aqueous solutions of peptide in the presence of Ni^{2+} and Co^{2+} ions display absorption spectra characteristic of tris-bipyridyl–metal complexes. For example, when complexed to Ni^{2+}, the intraligand π–π^* absorption bands of the bipyridine moiety occurring at 244 and 290 nm undergo a characteristic bathochromic shift with concomitant splitting of the longer wavelength band to 304 and 314 nm (ref 12) (Figure 3). Furthermore, size exclusion chromatography of the peptide under native or denaturing conditions and in the presence and the absence of Co^{2+} and Ni^{2+} was also shown to be consistent with the formation of a trimer in the presence of these ions (Figure 4). Although the labile nature of Ni^{2+} and Co^{2+} peptide complexes precluded their analysis by FIB MS (ref 13), $[Ru(bpy\text{-}peptide)_3]^{2+}$ which is a kinetically exchange inert complex gave a mass spectrum with a peak corresponding to the expected molecular mass ion at m/z = 5563 (Figure 5).

While the above studies suggest that the oligomeric state of an amphiphilic polypeptide may be simply defined by the interaction of a metal ion with a suitably designed metal binding site, the following experiments strongly support that the overall topology of the ensuing aggregate may also be controlled in the same step. In an amphiphilic peptide, such as the one used in this study, secondary structure is stabilized mainly through intermolecular hydrophobic interactions.[4,14] In other words, the formation of an intermolecular ensemble should be accompanied by an increase in the secondary structure content. Indeed, the α-helical content of the peptide increases dramatically in the presence of Ni^{2+} or Co^{2+} ions as evidenced by CD spectroscopy.[15] The peptide (7.4 μM in 5 mM sodium borate, pH 6.4, 21 °C) in the absence of added transition metal ions is only 30% α-helical ($[\theta]_{222} = -10{,}000$ deg·cm^2·dmol^{-1}), but in the presence of Ni^{2+} or Co^{2+} ion under similar conditions it exhibits >70% α-helicity ($[\theta]_{222} = -23400$ deg·cm^2·dmol^{-1})[16] (Figure 6). The α-helical structure can be further stabilized (80%, $[\theta]_{222} = -25800$ deg·cm^2·dmol^{-1}) in the presence of 150 mM NaCl. The fact that in the presence of a metal ion a trimeric structure with a high α-helical content was formed indicates that the peptide has undergone a metal ion-assisted intermolecular self-assembly process. Considering that the formation of a tris-bipyridyl–metal complex necessarily draws the N-termini of three peptides close in space, there are only two possible modes for interstrand helix–helix interactions which can bring about such dramatic secondary structure induction (Figure 7). Either the desired triple-helical coiled-coil topology is formed with the hydrophobic surface of each helix engaged with the neighboring helices or only two peptide subunits in the tris-bipyridine complex interact to form a two-stranded helical coiled-coil structure with the third subunit adopting a random orientation in solution. These two possibilities can be easily distinguished by measuring the dependence of secondary structure induction on the metallopeptide concentration. The triple helical structure lacking a solvent exposed hydrophobic surface should show CD spectra independent of the metallopeptide concentration, while the double-stranded structure having an unmatched amphiphilic peptide available for further intermolecular interaction should display concentration dependent CD spectra. As shown in Figure 8, the α-helical content of the peptide in the presence of Co^{2+} remains constant in the measured range of 5 to 300 μM peptide concentration, indicating that the desired triple-stranded topology is formed (Figure 9). Similar behavior was observed for the Ni(II) and Ru(II) complexes. It is also interesting to note that the peptide in the absence of added metal ions undergoes concentration dependent intermolecular aggregation to form, surprisingly, a dimeric structure (legend to Figure 8). Such behavior further illustrates the utility of metal ions in redirecting or overriding the intrinsic preference of the peptide for the formation of intermolecular structure(s) by selectively stabilizing the triple-helical topology even though the desired ensemble apparently is not the thermodynamically most stable entity in the absence of metal ions.

Furthermore, since tris-bipyridyl–metal complexes are chiral and can form either the left-handed Λ or right-handed Δ isomer, a priori, there are two diastereomeric triple-helical structures possible (Figure 10). However, the stereogenic environment of the ensuing parallel triple-helical topology as well as the geometrical constraints imposed by the overall C_3 symmetry of the structure was expected to enforce a high degree of diastereoselectivity in the assembly process. Indeed, the CD spectrum of the $[Ni(bpy\text{-}peptide)_3]^{2+}$ in the 280–330-nm region indicates formation of one diastereomer in which the tris-bipyridyl moiety adopts a left-handed Λ-isomer[12] (Figure 11). Such behavior is also consistent with the expected left-handed supercoil of the helical coiled-coil structure.[7,17]

Interestingly, the triple-helical metalloproteins display cooperative guanidine hydrochloride denaturation curves with a transition near 2 M GdnHCl (Figure 12). The analysis of the

(14) (a) Kauzmann, W. *Adv. Protein Chem.* **1959**, *14*, 1. (b) Radzicka, A.; Wolfenden, R. *Biochemistry* **1988**, *27*, 1664. (c) Rose, G. D.; Geselowitz, A. R.; Lesser, G. J.; Lee, R. H.; Zehfus, M. H. *Science* **1985**, *229*, 834 and references cited therein. (d) Eisenberg, D.; McLachlan, A. D. *Nature* **1986**, *319*, 199.

(15) (a) Woody, R. W. In *The Peptides*; Udenfriend, S.; Meienhofer, J., Eds.; Academic Press Inc.: New York, 1985; Vol. 7, p 15. (b) Greenfield, N.; Fasman, G. D. *Biochemistry* **1969**, *8*, 4108. (c) Johnson, W. C., Jr. *Annu. Rev. Biophys. Chem.* **1988**, *17*, 145.

(16) Bipyridine–metal complexes do not have a significant contribution to the CD spectrum below 250 nm as judged by comparing the CD spectra of heat and guanidine hydrochloride denatured metallopeptide complexes to the CD spectrum of uncomplexed peptide under similar conditions. For 100% helix the value of $[\theta]_{222} = -32000$ deg·cm^2·dmol^{-1} was used. See: Chen, Y.; Yang, J.; Chau, K. *Biochemistry* **1974**, *13*, 3350.

(17) Schulz, G. E.; Schirmer, R. H. *Principles of Protein Structure*; Springer: Berlin, 1979. See also ref 1.

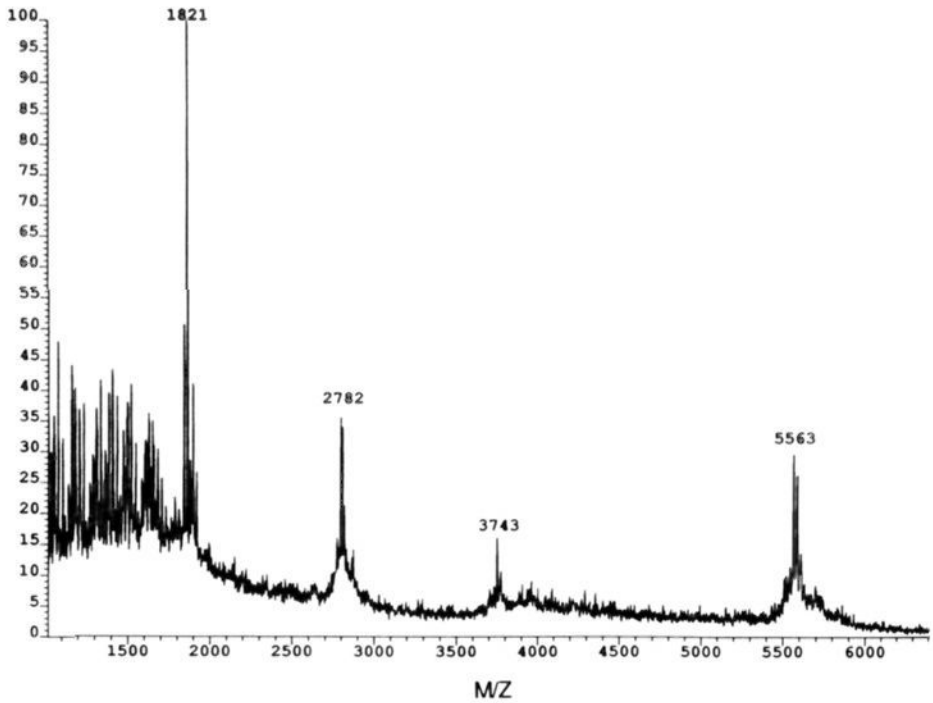

Figure 5. FIB positive ion mass spectrum of Ru(bpy-peptide)$_3^{2+}$ obtained on a VG ZAB-VSE double focusing mass spectrometer equipped with a cesium ion gun. The peaks at 5563 and 2782 correspond to m/z and $m/2z$ ions of the intact molecule, respectively. The peak at 3743 corresponds to the loss of one peptide subunit, and the peak at 1821 corresponds to the bpy-peptide.

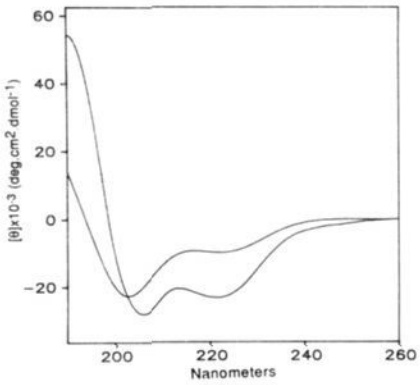

Figure 6. CD spectra of bpy-peptide (7.4×10^{-6} M in 5 mM sodium borate, pH 6.4 at 20.8 °C). Top curve at 222 nm is the peptide in the absence of transition metal ions and the bottom curve is in the presence of 9.8×10^{-6} M $NiCl_2$.

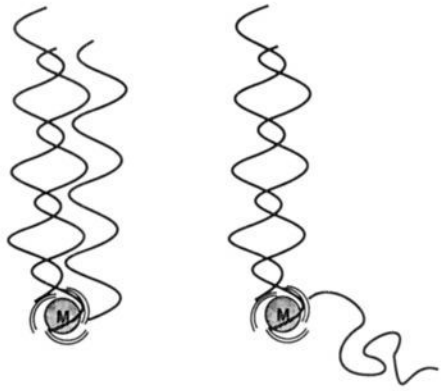

Figure 7. Schematic representation of the two possible topologies in the self-assembly process.

denaturation curves for the Ni(II) and the exchange-inert Ru(II) metalloproteins indicates the free energy of stabilization $\Delta G(H_2O)_{Ru} = 1.86 \pm 0.15$ kcal·mol^{-1}, $m = 950 \pm 69$ cal·mol^{-1}·M^{-1}

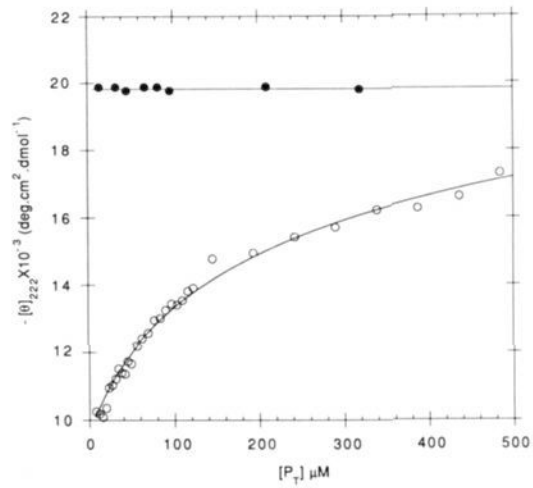

Figure 8. Plot of the concentration dependence of the ellipticity of bpy-peptide at 222 nm: (●) peptide plus 2.5 equiv of $CoCl_2$; (○) peptide in the absence of added metal ions at various concentrations. Data (○) were analyzed according to monomer–n-mer equilibria using the equation described below,[2d] where P_n, P_{mon}, and P_T are the self-associated, mo-

$$[P_T] = \left\{ \frac{(\theta_{obs} - \theta_{mon})K_{diss}}{n(\theta_n - \theta_{mon})(1 - ((\theta_{obs} - \theta_{mon})/(\theta_n - \theta_{mon})))^n} \right\}^{1/(n-1)}$$

nomeric, and total concentrations of the peptides, respectively, n is the degree of association, θ_{obsd} is the ellipticity observed at 222 nm, θ_{mon} is the ellipticity of the monomer, and θ_n is the ellipticity of the self-associated form of the peptide. The values of $n = 1.93$, $\theta_{mon} = -9500$, $\theta_n = -24900$, and $K_{diss} = 8.5 \times 10^{-4}$ were determined by the nonlinear regression program MINSQ.

and $\Delta G(H_2O)_{Ni} = 1.93 \pm 0.10$ kcal·mol^{-1}, $m = 1012 \pm 49$ cal·mol^{-1}·M^{-1}, respectively.[18,19] The observed near 2 kcal·mol^{-1}

(18) (a) Pace, N. C. *Trends Biotechnol.* **1990**, *8*, 93 and references cited therein. (b) Santoro, M. M.; Bolen, D. W. *Biochemistry* **1988**, *27*, 8063. (c) Pace, N. C.; Shirley, B. A.; Thomson, J. A. In *Protein Structure*; Creighton, T. E., Ed.; IRL Press: Oxford, 1989; p 311.

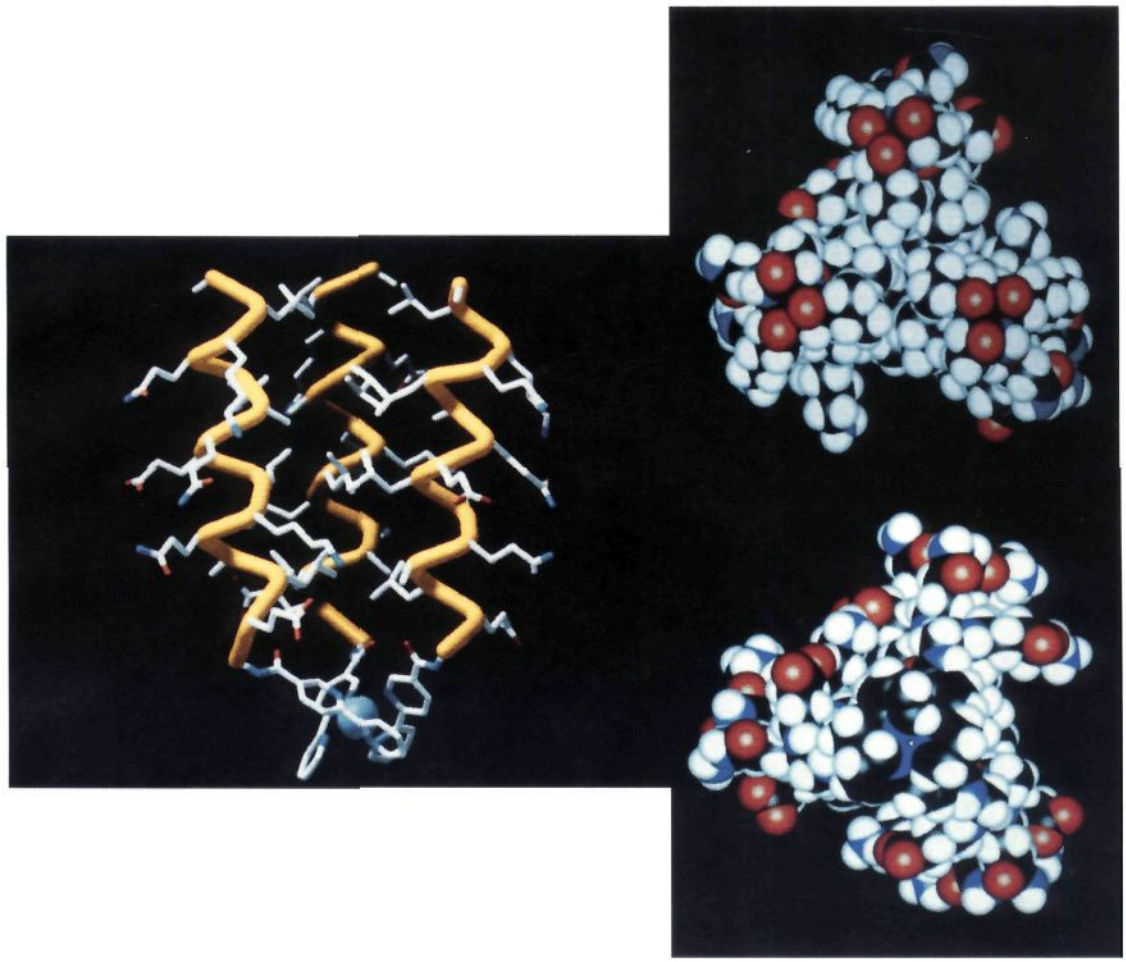

Figure 9. Computer generated model of metal ion-assisted triple-helical coiled-coil protein: (A, left) side view of the structure with the helical backbone and the bipyridyl metal binding site; (B, top right, and C, bottom right) top and bottom views shown in a space filling representation.

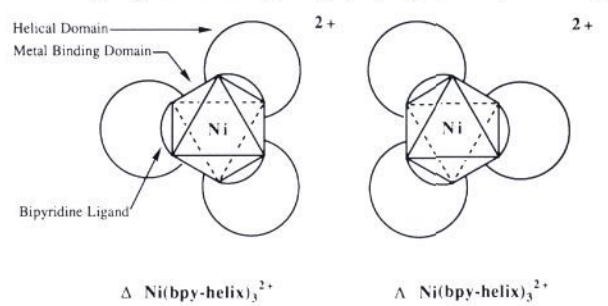

Figure 10. Schematic representation of the two possible diastereomers in the assembly of the triple-helical metalloprotein.

stability for these metalloprotein constructs is remarkable considering the low solvent-excluded hydrophobic surface area of the short triple-stranded coiled-coil structure. Optimization of the hydrophobic packing interactions as well as increasing the length of helical segments should provide further structural stability.

In summary, we have shown that a convergent metal ion-assisted self-assembly process can be a simple and effective method for the design and construction of a topologically predetermined protein structure.

(19) A series of studies using size exclusion chromatography, Superose 12 HR 10/30 column (Pharmacia), were used to find the optimum metal ion concentration for the formation of Ni(II) triple helical metalloprotein. Furthermore, tris-bipyridylpeptide complex was found to be stable under the GndHCl denaturation studies and no detectable dissociation was observed in the measured range of 0 to 6 M GndHCl concentrations. This observation is further supported by the nearly identical denaturation curves (figure 12) for the Ni(II) and the exchange-inert Ru(II) metalloproteins.

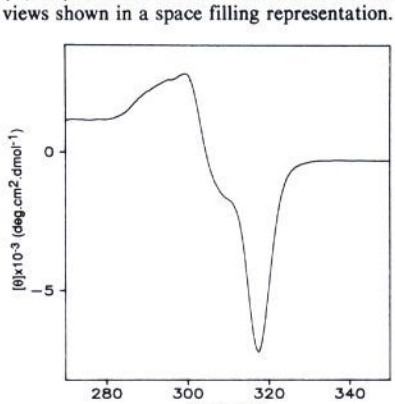

Figure 11. CD spectrum of bpy-peptide (38×10^{-6} M in 5 mM sodium borate, pH 6.1 at 20.8 °C) in the presence of 56×10^{-6} M $NiCl_2$.

Experimental Section

Proton nuclear magnetic resonance spectra were recorded at 300 MHz on a Bruker AM300 spectrometer and are reported in parts per million (ppm) downfield from Me_4Si. Ultraviolet–visible spectra were recorded on Aviv Associates 14DS and Milton Roy Spectronic 3000 Array spectrometers. Circular dichroism measurements were made on an Aviv Associates 62DS spectrometer equipped with a thermostatable cell holder using 10-, 1-, and 0.1-mm Hellma quartz cells. All ellipticity measurements are expressed as mean residue ellipticity, $[\theta]$, having the units deg·cm^2·dmol^{-1}. Peptide concentrations were determined by quantitative amino acid analysis (average of three runs) using norleucine as internal standard. All reported CD data have an uncertainty of ±2–5%. The FIB positive ion mass spectra were obtained on a VG ZAB-VSE double focusing mass spectrometer equipped with a cesium ion gun. 4-

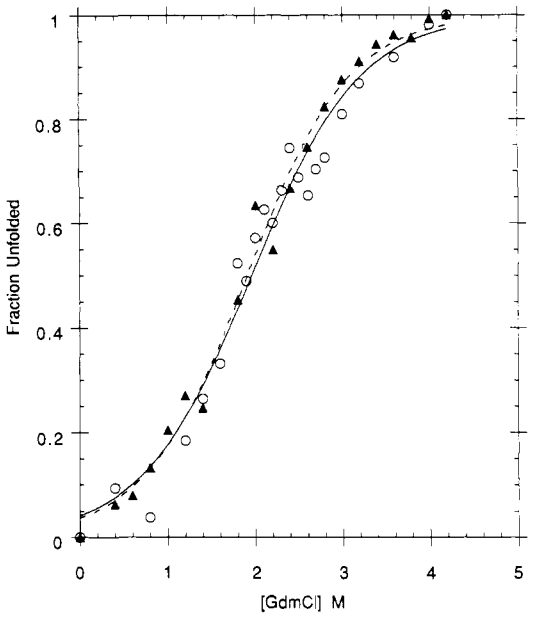

Figure 12. Guanidine hydrochloride denaturation curves for (▲) Ni(II) and (○) Ru(II) triple-helical metalloproteins (0.45 mM, in 100 mM HEPES, pH 7.0) measured by CD at 222 nm. Solid and broken lines are based on the parameters obtained by a nonlinear least-squares fit of the data for Ru(II) and Ni(II) metalloproteins, respectively, to eq 2 described in the Experimental Section.

Methylbenzhydrylamine resin (0.65 mequiv/g 150–200 mesh) and blocked amino acids used in peptide synthesis were obtained from Advanced Chemtech, Louisville, KY. HF cleavage was performed using a single-vessel apparatus purchased from Immuno-Dynamics Inc., La Jolla, CA. All high-purity solvents were purchased from Fisher Scientific except for the HPLC grade acetonitrile which was purchased from VWR Scientific. BOP reagent was obtained from Richelieu Biotech Inc., St.-Hyacinthe, Canada. All other chemicals were purchased from Aldrich. Diisopropylethylenediamine was distilled from potassium hydroxide under argon. Preparative reversed-phase HPLC was performed on a 2.2 × 25 cm Vydac C_4 (10-μm particle size) column using a binary gradient of (A) 1% acetonitrile/water/0.1% TFA and (B) 90% acetonitrile/water/0.07% TFA. Elution profiles were monitored at 225 and 280 nm. Analytical reversed-phase HPLC was done using a 4.6 × 250 mm Vydac C_{18} (5-μm particle size) column using the above binary gradient.

Guanidine hydrochloride denaturation curves were determined by measuring the mean residue ellipticity at 222 nm on an Aviv Associates 62DS spectrometer of solutions containing 450 μM metalloprotein in 100 mM HEPES buffer pH 7.0 as a function of GndHCl concentration in a thermostated 0.1-mm Helma quartz cell. The solutions were kept at 25 °C for 1 h or more before measurements were made. Each reported data point is the average of sixty consecutive measurements over a period of 1 min. Denaturation curves were analyzed using least-squares fit (nonlinear regression program MINSQ) to the following equation[18]

$$f_u = (\exp[-(\Delta G(H_2O)/RT - m[D]/RT)])/(1 + \exp[-(\Delta G(H_2O)/RT - m[D]/RT)]) \quad (2)$$

where $f_u = (\theta_n - \theta_{obs})/(\theta_n - \theta_d)$ is the fraction unfolded, [D] is the denaturant concentration, m is the measure of dependence of ΔG on denaturant concentration, θ_n is the measured $[\theta]_{222}$ for the native conformation, θ_d is the measured $[\theta]_{222}$ for the denatured conformation, and θ_{obs} is the observed variable parameter.

Preparation of 5-Carboxy-2,2′-bipyridine.[20] A solution of 2-chloro-5-ethylnicotinate (2 g, 10.8 mmol), 2-trimethylstannylpyridine[21] (2.7 g, 11.3 mmol), and $Pd(Ph_3P)_2Cl_2$ (0.4 g, 0.54 mmol) in dry THF (15 mL) was refluxed for 20 h. The brown reaction mixture was evaporated, taken up in dichloromethane, and filtered through a silica gel–Celite bed. Evaporation of solvent gave 5-(ethoxycarbonyl)-2,2′-bipyridine as a pale yellow solid (1.3 g, 54%). The crude material was >95% pure as judged by ^{1}H NMR and thin layer chromatography and was used in the next reaction without further purification. ^{1}H NMR ($CDCl_3$, 300 MHz) δ 1.43 (t, J = 7 Hz, 3 H, CH_3CH_2), 4.43 (q, J = 7 Hz, 2 H, CH_2CH_3), 7.36 (m, 1 H), 7.84 (m, 1 H), 8.42 (m, 1 H), 8.50 (m, 2 H), 8.70 (d, J = 4.2 Hz, 1 H), 9.27 (d, J = 1.5 Hz, 1 H). MS (FIB) $(M + H)^+$ = 229. The crude ester (1 g, 4.4 mmol) was then taken up in methanol (5 mL) to which was added 1 N NaOH (5 mL) and the solution stirred at room temperature for about 3 h. Solvent was then evaporated and the residue dissolved in a minimum amount of water. The solution was extracted with dichloromethane and the aqueous layer acidified to pH = 3 with concentrated HCl. The product precipitated as analytically pure white crystals (0.83 g, 95%). ^{1}H NMR (DMSO, 300 MHz) δ 7.36 (m, 1 H), 7.86 (m, 1 H), 8.45 (m, 3 H), 8.71 (d, J = 4 Hz, 1 H), 9.29 (s, 1 H). MS (FIB) $(M + H)^+$ = 201.

Peptide Synthesis. The peptide was prepared by employing *N-tert*-butyloxycarbonyl (Boc) amino acid derivatives for Merrifield solid-phase synthesis.[22] *N*-α-Boc-L-amino acids were used with the following side chain protecting groups: Glu(OBzl), Lys(Cl-Z). Manual peptide syntheses were carried out in a 30-mL vessel fitted with a coarse glass frit.[22b] Manual assembly of the protected peptide on the 4-methylbenzhydryl amine resin was carried out at room temperature using the following reaction step cycles. First the Boc protecting group was removed from the α-amino group of the resin-bound amino acid with TFA (50% TFA in CH_2Cl_2 for 1 and 20 min). The deprotected peptide resin was then neutralized with 10% DIEA in CH_2Cl_2 (2 × 2 min). Amino acids were coupled to the free α-amino group by the addition of 3 equiv of Boc-amino acid, 3 equiv of BOP reagent, and 5.3 equiv of DIEA in 10–15 mL of DMF.[23] The reaction was allowed to proceed for a total of 2 h. The coupling step was monitored by Kaiser test. If a second coupling was necessary, the resin was first neutralized with 10% DIEA in dichloromethane.

Coupling of 5-Carboxy-2,2′-bipyridine to the NH_2 Terminus of the Resin-Bound Peptide. A sample of peptide/resin (1.0 g, 0.23 mequiv/g) was placed in a 10-mL reaction vessel, and the resin was washed five times with dichloromethane. The terminal Boc protecting group was removed and the resin was neutralized by standard procedures. In a separate flask, 5-carboxy-2,2′-bipyridine (201 mg, 1.0 mmol), 1-hydroxybenzotriazole monohydrate (153.1 mg, 1.0 mmol), and 4-(dimethylamino)pyridine (30 mg, 0.25 mmol) were dissolved in 5.0 mL of DMF. To this solution diisopropylcarbodiimide (157 μL, 1.0 mmol) was added and the mixture stirred at room temperature for 30 min. The mixture was then transfered to the peptide/resin reaction vessel and allowed to react for 3–4 h (until negative kaiser test) with constant shaking. The resin was then washed with DMF (5×) and CH_2Cl_2 (5×) and dried in vaccuo.

Deprotection and Purification. Dried resin was placed in the HF apparatus. Side chain protecting groups as well as the peptide–resin bond were cleaved under "high HF" conditions (90% HF, 10% *p*-cresol) at 0 °C for 2 h.[24] After removal of HF under vacuum, the peptide–resin residue was placed on a fritted funnel and washed with diethyl ether (5×). The peptide was then dissolved in 10% aqueous acetic acid and filtered through, leaving the resin on the frit. The crude peptide solution was lyophilized and samples of 150–200 mg were redissolved in 2% aqueous acetic acid and subjected to gel filtration on a Sephadex G15 column (2 × 50 cm) preequilibrated with the same solvent to remove the scavenger and small molecular weight contaminants. The peptide was then purified by preparative reversed-phase HPLC on a Vydec C_4 column using a 20-min linear gradient of 22–63% acetonitrile/water/0.1% TFA with a 9.0 mL/min flow rate. The desired peptide fraction (18-min retention time) was collected, lyophilized, and characterized by amino acid analysis and FIB mass spectroscopy (m/z = 1821). Analytical RP HPLC indicated that the gel-filtered crude peptide was >90% pure and the HPLC purified samples >99% pure.

Preparation of Tris(2,2′-bipyridyl peptide)ruthenium(II) Complex. Ruthenium trichloride hydrate (0.7 mg, 3.3 μmol) under an argon atmosphere was dissolved in 100 μL of a degassed 50% ethanol–water mixture in a 1.0-mL Schlenk-type tube. The reaction mixture was heated at 90 °C for 30 min during which time the color of the solution changed from brown to green to dark blue. Bipyridyl peptide (20 mg, 11 μmol) was dissolved in 100 μL of a degassed 50% ethanol–water mixture and added to the ruthenium "blue" solution under an argon atmosphere. The heating was continued for an additional 30 min. As the reaction progressed the solution turned from deep blue to reddish brown. The reaction

(20) For the synthesis of unsymmetrical heterobiaryls see: Bailey, T. R. *Tetrahedron Lett.* **1986**, *27*, 4407.

(21) Jutzi, P.; Gilige, U. *J. Organomet. Chem.* **1983**, *246*, 163.

(22) (a) Barany, G.; Merrifield, R. B. In *The Peptides*; Udenfriend, S., Meienhofer, J., Eds.; Academic Press Inc.: New York, 1979; Vol. 2, p 3. (b) *Solid Phase Peptide Synthesis*; Stewart, J. M., Young, J. D., Eds.; Pierce Chemical Co.: Rockford, MD, 1984.

(23) (a) Hudson, D. *J. Org. Chem.* **1988**, *53*, 617. (b) Castro, B.; Dormoy, J. R.; Evin, E.; Orura, H. *Tetrahedron Lett.* **1975**, 1219.

(24) (a) Tam, J. P.; Merrifield, R. B. In *The Peptides*; Udenfriend, S., Meienhofer, J., Eds.; Academic Press Inc.: New York, 1987; Vol. 9, p 185.

(25) **Note Added in Proof**: After the submission of this manuscript, a preliminary report describing a similar approach to ours was reported. Lieberman, M.; Sasaki, T. *J. Am. Chem. Soc.* **1991**, *113*, 1470.

mixture was allowed to cool to room temperature and directly applied to a Sephadex G-25 gel filtration column and elluted with water. The desired metalloprotein complex was then separated from the small amounts of unreacted peptide using ion exchange chromatography on CM-Sephadex C-25 with a 0-2 M NaCl salt gradient in 50 mM MES pH 6.5 buffer. Final purification as well as desalting was performed using RP HPLC to afford about 15 mg of the desired metalloprotein. Formation of the desired complex was established by FIB mass spectroscopy m/z = 5563 (Figure 5) and the following characteristic ultraviolet and visible absorption bands: λ_{max} (nm) 255, 300, and 470 br.

Acknowledgment. The Searle Scholars Program/The Chicago Community Trust and the Arnold and Mabel Beckman Foundation are gratefully acknowledged for their support for of this work. We are also grateful to Dr. C. Singh and V. N. Balaji for the computer-generated model, M. Pique for the graphics presentation, Dr. G. Siuzdak for mass spectroscopic analysis, and colleagues B. Oskouian for help in the design and R. Lerner, K. C. Nicolaou, P. Wright, L. Walters, and J. Skolnick for valuable discussions.

Registry No. 2,2'-Bipyridyl-5-carbonyl-GELAQKLEQALQKLA-NH_2, 138060-62-5; ethyl 6-chloronicotinate, 49608-01-7; 2-(trimethylstannyl)pyridine, 13737-05-8; 5-(ethoxycarbonyl)-2,2'-bipyridine, 56100-24-4; 5-carboxy-2,2'-bipyridine, 1970-80-5.

Resonance Interactions in Acyclic Systems. 3. Formamide Internal Rotation Revisited. Charge and Energy Redistribution along the C-N Bond Rotational Pathway

Kenneth B. Wiberg* and Curt M. Breneman†

Contribution from the Department of Chemistry, Yale University, New Haven, Connecticut 06511.
Received January 24, 1991

Abstract: The changes that occur during the rotation of the amino group of formamide have been studied in some detail. Geometry optimizations at the MP2/6-31G* level confirmed the relatively large increase in C-N bond length but small decrease in the C-O length on going from the planar structure to the rotational transition state. A calculation of the force constants for formamide and for the transition state showed that the carbonyl force constant changed relatively little, but the C-N constant changed by about 30%. The path followed in the rotation was studied starting with the saddle point geometry and following it computationally down to the ground state. The geometrical changes are discussed. The electron populations were calculated for a number of structures along the reaction coordinate by numerical integration of the charge density within uniquely defined atomic volumes. The oxygen population was little affected by the rotation and the main charge shift was between carbon and nitrogen. The electrostatic potentials for the structures also were examined and converted to effective charges for spherically symmetrical atoms. All of the analyses indicated that essentially all of the interactions leading to the rotational barrier originate in the C-N bond and that the oxygen does not participate to a significant extent. The direction of the charge shift between C and N was in opposite directions for the electron populations derived by integration of the charge density, and by fitting the electrostatic potentials. However, this was due to the difference in the definition of the atoms, being anisotropic in the first case and spherically symmetrical in the second. All of the observations can be rationalized on the basis of the assumption that stabilization of the lone pair on nitrogen is the most important factor in determining both structures and energies.

1. Introduction

The amide group is one of the most important functional groups in chemistry. Its planarity and relatively high barrier to rotation about the C-N bond are important factors in determining the conformations of peptides and related compounds. Most of the properties of amides are readily rationalized by postulating amide resonance of the type

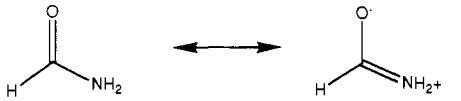

Invocation of partial double bond character for the C-N bond allows one to account for the rotational barrier, since this presumably stabilizing interaction would be lost when the amino group is rotated by 90°. Similarly, planarity of the amino group would be required in order to achieve a maximum resonance interaction. Addition of a nucleophile to the carbonyl group would result in loss of the resonance interaction, and so one would correctly predict that these additions would be unfavorable. The resonance interaction model also provides a convenient explanation for the observed stabilization achieved by the combination of an amino group and a carbonyl group. The magnitude of this interaction can be estimated from the following hypothetical reaction (kcal/mol)[1]

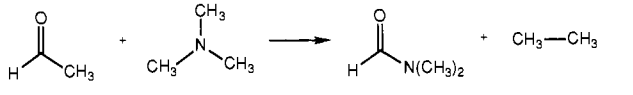

ΔH_f = −39.37 ΔH_f = −5.67 ΔH_f = −45.8 ΔH_f = −20.24

$\Delta\Delta H$ = −21.0 kcal/mol

The energy change is close to that for the rotational barrier, indicating that the corresponding reaction forming the 90° rotated structure would be close to thermoneutral.

Despite the success of the above resonance picture in explaining a large body of data, there are some observations which cast doubt on this simple interpretation. In an earlier investigation of the rotational barrier in formamide, in which the observed barrier was successfully reproduced via ab initio molecular orbital calculations using the 6-31G** basis set, the changes in electron population and structure on rotation were found not to be in accord with an electron donation from the amino group to the carbonyl

† Present address: Department of Chemistry, Rensselaer Polytechnic Institute, Troy, NY 12180.

(1) Cox, J. D.; Pilcher, G. *Thermochemistry of Organic and Organometallic Compounds*; Academic Press: New York, 1970.

0002-7863/92/1514-831$03.00/0 © 1992 American Chemical Society